

Development-related mitochondrial properties of retinal pigment epithelium cells derived from hEROs

Hao-Jue Xu^{1,2}, Qi-You Li^{1,2}, Ting Zou^{1,2}, Zheng-Qin Yin^{1,2}

¹Southwest Hospital/Southwest Eye Hospital, Third Military Medical University (Army Medical University), Chongqing 400038, China

²Key Lab of Visual Damage and Regeneration & Restoration of Chongqing, Chongqing 400038, China

Correspondence to: Ting Zou and Zheng-Qin Yin. Southwest Hospital/Southwest Eye Hospital, Third Military Medical University (Army Medical University), Chongqing 400038, China. zoutingcq@163.com; qinzyin@aliyun.com

Received: 2021-02-04 Accepted: 2021-06-21

Abstract

• **AIM:** To explore the temporal mitochondrial characteristics of retinal pigment epithelium (RPE) cells obtained from human embryonic stem cells (hESC)-derived retinal organoids (hEROs-RPE), to verify the optimal period for using hEROs-RPE as donor cells from the aspect of mitochondria and to optimize RPE cell-based therapeutic strategies for age-related macular degeneration (AMD).

• **METHODS:** RPE cells were obtained from hEROs and from spontaneous differentiation (SD-RPE). The mitochondrial characteristics were analyzed every 20d from day 60 to 160. Mitochondrial quantity was measured by MitoTracker Green staining. Transmission electron microscopy (TEM) was adopted to assess the morphological features of the mitochondria, including their distribution, length, and cristae. Mitochondrial membrane potentials (MMPs) were determined by JC-1 staining and evaluated by flow cytometry, reactive oxygen species (ROS) levels were evaluated by flow cytometry, and adenosine triphosphate (ATP) levels were measured by a luminometer. Differences between two groups were analyzed by the independent-samples *t*-test, and comparisons among multiple groups were made using one-way ANOVA or Kruskal-Wallis *H* test when equal variance was not assumed.

• **RESULTS:** hEROs-RPE and SD-RPE cells from day 60 to 160 were successfully differentiated from hESCs and expressed RPE markers (Pax6, MITF, Bestrophin-1, RPE65, Cralbp). RPE features, including a cobblestone-like morphology with tight junctions (ZO-1), pigments and microvilli, were also observed in both hEROs-RPE and SD-

RPE cells. The mitochondrial quantities of hEROs-RPE and SD-RPE cells both peaked at day 80. However, the cristae of hEROs-RPE mitochondria were less mature and abundant than those of SD-RPE mitochondria at day 80, with hEROs-RPE mitochondria becoming mature at day 100. Both hEROs-RPE and SD-RPE cells showed low ROS levels from day 100 to 140 and maintained a normal MMP during this period. However, hEROs-RPE mitochondria maintained a longer time to produce high levels of ATP (from day 120 to 140) than SD-RPE cells (only day 120).

• **CONCLUSION:** hEROs-RPE mitochondria develop more slowly and maintain a longer time to supply high-level energy than SD-RPE mitochondria. From the mitochondrial perspective, hEROs-RPE cells from day 100 to 140 are an optimal cell source for treating AMD.

• **KEYWORDS:** mitochondria; retinal organoids; retinal pigment epithelium cells; human embryonic stem cells, retinal degenerative diseases

DOI:10.18240/ijo.2021.08.02

Citation: Xu HJ, Li QY, Zou T, Yin ZQ. Development-related mitochondrial properties of retinal pigment epithelium cells derived from hEROs. *Int J Ophthalmol* 2021;14(8):1138-1150

INTRODUCTION

Age-related macular degeneration (AMD) is a retinal degenerative disease that results in permanent visual impairment^[1] and is the premier cause of blindness in developed countries^[2]. The incidence rate of AMD in developing countries has increased continuously in recent decades, with 8.7% of the worldwide population currently suffering, and 288 million projected to be affected by 2040^[3]. Specifically, the projected number of people with AMD in China is approximately 31.23 million, which is astounding^[4]. Individuals with AMD, in addition to physical harm^[5], also bear mental distress due to their impaired vision^[6-9].

During the development of AMD, retinal pigment epithelium (RPE) cells are damaged first, followed by photoreceptor death, and severe neuroretinal degeneration and choroid atrophy can occur^[10]. However, current therapeutic strategies are intended to control the symptoms and delay the progression

of degeneration^[11]. Stem cell therapy is a promising method for treating AMD, and RPE cells derived from human embryonic stem cells (hESCs-RPE) in spontaneous differentiation (SD) have been investigated in several clinical trials in different regions for the treatment of AMD^[12-18]. The results have shed light on methods for easing the effects of vision loss on affected individuals and their families as well as on society. In these trials, the safety and efficiency of hESC-RPE cells were proven preliminarily. Additionally, our group previously demonstrated that the subretinal injection of hESCs-RPE cells was safe for patients with wet-AMD within a 12-month follow-up period^[15]. How to obtain the best cell source for RPE transplantation has remained a concern until now.

Notably, SD-RPE cells were used in the clinical trials described above. Excitingly, hESCs can be differentiated into retinal organoids (hEROs), further simulating retinal development *in vivo*^[19], and this protocol is widely applied in disease model establishment and stem cell-based therapies^[20-21]. Various retinal organoids-derived cells have been reported and shown to exhibit a better profile than their SD counterparts^[22-23]. We previously compared the differences between retinal organoids-derived RPE (hEROs-RPE) and SD-RPE cells^[22], revealing that hEROs-RPE cells were less mature than SD-RPE cells and were advantageously more proliferative and exhibited a better ultrastructure, tight junction, and polarity. hEROs-RPE cells are quite similar to human fetal RPE cells (hFRPE) since the induction of retinal organoid mimics the normal development process of embryonic retinal tissue *in vivo*. However, additional features of hEROs-RPE cells including their mitochondria, during development have not been characterized.

While the mechanisms of stem cell-based therapy remain elusive, transplanted stem cells were previously shown to protect or generate retinas during retinal degeneration *via* cell replacement. Recently, cellular exchange between donor stem cells and host retinal cells has received increased attention as a new donor and crucial mechanism^[24-25]. Our previous results also showed that organoids-derived human retinal progenitor cells could protect against retinal degeneration *via* the transfer of materials between donor cells and recipient photoreceptors^[26]. Thus, the mechanism and content of cellular exchange are being explored.

In particular, the mitochondrial transfer has recently become a popular research topic because of the cellular “powerhouse” status of these organelles, which are responsible for cellular metabolism and energy production^[27]. Additionally, similar to those with other degenerative diseases^[28], patients suffering from AMD exhibit analogical pathologies, including mitochondrial dysfunction^[29-30]. Previous studies reported that transferred healthy mitochondria were capable of rescuing an undesirable metabolic status^[31-33]. Moreover, a previous study

showed that healthy ARPE19 cells could transfer mitochondria to healthy RPE cells *in vitro*, confirming the possibility of mitochondrial transfer^[34]. Predictably, treating AMD *via* the transfer of mitochondria from transplanted hESC-RPE cells to recipient RPE cells is promising, and more explorations are needed to determine the optimal conditions for obtaining hESC-RPE cell mitochondria during the developmental process. The mitochondrial characteristics of hESC-RPE cells, including their quantity and quality, urgently need to be elucidated^[34].

Since mitochondrial transfer is an important mechanism of stem cell therapy and the induced period for hESC-RPE cells is long, determining the appropriate time window for obtaining hESC-RPE cells with high-quality mitochondria would be very significant. In this study, we compared the morphological and functional characteristics of mitochondria from hEROs-RPE and SD-RPE cells from day 60 to 160, aiming to determine the optimal time window for RPE cell screening from the perspective of mitochondria and thus providing additional evidence for improving stem cell therapy for AMD therapies.

MATERIALS AND METHODS

Differentiation of hEROs-RPE and SD-RPE Cells A clinical-grade hESC line (Q-CTS-hESC-2)^[35] was used as the cell source to induce RPE cells. For hEROs-RPE cell differentiation, hESCs formed embryoid body-like aggregates in low-cell-adhesion 96-well plates with V-bottomed conical wells according to the protocol established by Sasai with slight modifications^[36]. In short, hESCs were digested into single cells with TrypLE Express (12605028, Thermo Fisher Scientific, USA) and 1.2×10^4 cells/well were resuspended in growth factor-free chemically defined medium (gfCDM) containing 20 $\mu\text{mol/L}$ Y-27632 (1293823, Peprotech-BioGems, USA). The cells were then seeded into 96-well V-bottomed conical wells with low-cell-adhesion (100 $\mu\text{L/well}$) and cultured in 5% CO_2 at 37°C. gfCDM was supplemented with 10% knockout serum replacement (kOSR, 12618013, Thermo Fisher Scientific, USA), 45% Iscove’s modified Dulbecco’s medium (IMDM, 12440-053, Gibco, USA), 45% Hams F12 medium (F12, 31765-035, Gibco, USA), 1% GlutaMAX (A12860-01, Gibco, USA), 1% chemically defined lipid concentrate (11905-031, Gibco, USA), and monothioglycerol (450 mmol/L, M6145, Sigma, USA). The time of inoculation into V-bottomed conical wells was defined as day 0. The gfCDM contained recombinant human BMP4 (AF-120-05ET, Peprotech, USA) at a final concentration of 1.5 nmol/L (55 ng/mL) on day 6, and the BMP4 concentration was diluted by 50% with gfCDM every 3d until day 18. The embryoid body-like aggregates were transferred from the 96-well plate to a 10-cm low-adhesion Petri dish and further suspended and cultured in RPE long-term differentiation medium. This medium was

comprised of basic DMEM/F12-GlutaMAX medium (10565-018, Gibco, USA) and 1% N2 (A1370701, Gibco, USA) and was supplemented with 3 $\mu\text{mol/L}$ glycogen synthase kinase-3 inhibitor (GSK3i, 2520691, Biogems) and 5 $\mu\text{mol/L}$ fibroblast growth factor receptor inhibitor (FGFRi, 2159233, Biogems) on day 18 and 24 and supplemented with 1% (FBS) and 3 $\mu\text{mol/L}$ GSK3i after day 24; the culture medium was completely replaced every 3d until the pigment cells were separated. The pigment clumps were mechanically separated and seeded onto a well precoated with truncated human Vitronectin (rhVTN, A14700, Gibco, USA). The time at which pigment foci were inoculated into the well plate was redefined as day 0. New RPE cells adhered to the plate and were subcultured and expanded every 20d.

The protocols for SD-RPE cell differentiation were described previously^[22,37]. In brief, the differentiation of superfused hESCs into RPE cells was induced in differentiation medium without basic fibroblast growth factor (bFGF). The formation of RPE cells was observed in approximately 40d, and the cells were mechanically separated and seeded into well plates precoated with rhVTN. The time at which the pigment foci were inoculated into the well plate was defined as day 0. Newborn RPE cells grew adherently from the edges of the separated RPE pigment foci and were subcultured and expanded every 20d.

RPE cells were cultured in Knock Out DMEM CTS (KO-DMEM, A1286101, Invitrogen, USA), 20% Knock Out SR xeno-free CTS (CTS-KOSR, 12618013 Invitrogen, USA), 1% nonessential amino acid solution (MEM NEAA, 11140-050, Gibco, USA), 1 mmol/L CTS GlutaMAX-1 supplement (A12860-01, Invitrogen, USA), and 1% 0.1 mmol/L β -mercaptoethanol (21985023, Gibco, USA).

Immunofluorescence and Confocal Microscopy Analyses of hESC-RPE Cells Cells cultured on a 10-mm glass slide for approximately 20d were fixed with 4% paraformaldehyde (PFA) for 20min, permeabilized with 0.5% Triton X-100 in phosphate-buffered saline (PBS) for 15min, and blocked with 3% BSA and 5% goat serum for 60min. Primary antibodies against ZO-1 (13663, 1:400, CST, USA), Pax6 (ab5790, 1:200, Abcam, USA), mitf (MA5-14146, 1:200, Invitrogen, USA), Bestrophin-1 (ab14929, 1:200, Abcam, USA), RPE65 (ab13826, 1:50, Abcam, USA) and Cralbp (ab15051, 1:200, Abcam, USA) were diluted in the same blocking buffer. The samples were incubated overnight at 4°C and then incubated with a fluorescently coupled secondary antibody for 1h at 37°C. Fluorescent secondary antibodies (Alexa Fluor 488-conjugated goat anti-mouse, A28175, 1:500, Invitrogen; or Alexa Fluor 488-conjugated goat anti-rabbit, A27034, 1:500, Invitrogen, USA) were used for visualization. The nuclei were

stained with 4,6-diamidino-2-phenylindole (DAPI; Solarbio) for 7min, and fluorescence images were acquired with a confocal microscope (Leica SP5).

Transmission Electron Microscopy Briefly, hEROs-RPE and SD-RPE cells were digested, and approximately 1×10^6 hESC-RPE cells were centrifuged after resuspension in PBS at every time point. The cell mass was immersed in glutaraldehyde overnight, rinsed with buffer, postfixed with 1% osmium tetroxide for 2h, subjected to graded acetone dehydration, and infiltrated with a 50:50 mixture of acetone and resin for 3-4h. After 72h, the tissues were embedded in resin and polymerized at 60°C for 48h, and 60 nm sections were then cut and stained with 2% uranyl acetate for 20min and 0.5% lead citrate for 5min. The hESC-RPE cell ultrastructure was visualized with a Philips Tecnai 10 transmission electron microscope (TEM; Philips, Holland). All analyses were performed in a blinded and nonbiased manner. For morphometric analyses of mitochondria, images were acquired at different magnifications and then edited with Adobe Photoshop CC 14.0 $\times 64$ (Photoshop CC Software, USA).

MitoTracker Green Staining and Testing After digestion of hEROs-RPE and SD-RPE cells, approximately 5×10^5 hESC-RPE cells were centrifuged and resuspended in warm differentiation medium at every time point. The suspended cells were incubated with MitoTracker Green [MTG; Cell Signaling Technology (CST), 9074] at a final concentration of 5 $\mu\text{L/mL}$ for 30min at 37°C. The mean fluorescence intensity was measured by flow cytometry on the FITC channel.

Reactive Oxygen Species Measurement Reactive oxygen species (ROS) production in hEROs-RPE and SD-RPE cells was measured with an ROS Assay Kit (Beyotime, China) according to the manufacturer's instructions. Briefly, hEROs-RPE and SD-RPE cells were digested, and approximately 5×10^5 hESC-RPE cells were centrifuged and resuspended in warm differentiation medium at every time point. The suspended cells were incubated with 10 $\mu\text{mol/L}$ DCFH-DA for 20min at 37°C and then washed three times with warm serum-free DMEM. The mean fluorescence intensity was measured by flow cytometry on the FITC channel.

Mitochondrial Membrane Potential Measurement The mitochondrial membrane potentials (MMPs) of hEROs-RPE and SD-RPE cells were measured with a fluorescent probe specific for MMP from the JC-1 kit (Beyotime, China) according to the manufacturer's instructions. After the simultaneous digestion of hEROs-RPE and SD-RPE cells, approximately 5×10^5 hESC-RPE cells were centrifuged and resuspended in warm differentiation medium at every time point. The suspended cells were incubated with JC-1 at a final concentration of 2.5 $\mu\text{L/mL}$ for 20min at 37°C and then

washed three times with warm serum-free medium. The mean fluorescence intensity was measured by flow cytometry on the PE and FITC channels.

Adenosine Triphosphate Measurement The adenosine triphosphate (ATP) levels in hEROs-RPE and SD-RPE cells were measured on ice with a firefly luciferase-based ATP assay kit (Beyotime, China) according to the manufacturer's instructions. Luminance was measured with a multimode microplate reader (Varioskan flasher, Thermo Scientific, USA), and emitted light was linearly related to the ATP concentration. After the simultaneous digestion of hEROs-RPE and SD-RPE cells, the same number of hESC-RPE cells was centrifuged in warm differentiation medium at every time point and tested. Three independently repeated trials were performed.

Flow Cytometry Flow cytometry analysis of hESC-RPE cells was performed with a BD Canto2 flow cytometer, and 10 000 events were acquired. Data were analyzed with flow cytometry software (FlowJo 7.6.1).

Statistical Analysis Statistical analyses were conducted with GraphPad Prism version 8.0.0 for Windows (GraphPad Software, San Diego, California, USA, www.graphpad.com/GraphPad). Comparisons between two groups were performed by the independent-sample *t*-test, and comparisons among multiple groups were made with one-way ANOVA followed by Tukey's multiple comparison test or Kruskal-Wallis *H* test when equal variance was not assumed. All values are presented as the mean±(SEM), and *P*<0.05 was considered statistically significant.

RESULTS

Differentiation and Identification of hEROs-RPE Cells Immunohistochemistry analysis confirmed that hESCs expressed the pluripotency stem cell markers Nanog, OCT4, and SSEA4 (Figure 1A). Then hESCs were induced to differentiate towards RPE cells by two approaches, forming hEROs-RPE and SD-RPE cells, with SD-RPE cells as a control. During hEROs culture, hESCs formed embryonic bodies at day 6, and retinal organoids were formed at day 19 to 25; RPE cells were formed simultaneously (Figure 1B). We used retinal organoids from day 42-48 to produce abundant hEROs-RPE cells *via* the protocol established by Sasai with slight modifications^[36]. After continuous culture for three weeks, pigments gradually enlarged and formed foci. At day 42-48, these pigment foci were excised and placed onto 6-well plates to allow hEROs-RPE cells to expand and grow (Figure 1B). The time point at which hEROs-RPE cells were separated from the pigmented foci was defined as day 0. For SD-RPE cells, hESCs began to differentiate after superfusion, and pigment foci were observed after approximately 25d. After these pigmented lesions became sufficiently large on approximately day 45, they were mechanically separated and

continued to differentiate in a 6-well plate to allow for the continued expansion of SD-RPE cells. Similarly, this day was deemed day 0 of SD-RPE cell differentiation (Figure 1C).

Since we planned to assess hESC-RPE mitochondria from day 60 to 160, we confirmed the RPE markers (ZO-1, Pax6, MITF, Bestrophin-1, RPE65, Cralbp) in hEROs-RPE and SD-RPE cells at day 60 and 160 by immunohistochemistry analysis (Figure 1D). Pigments and cobblestone-like morphology were observed through bright field microscopy, verifying that we obtained RPE cells *via* both differentiation methods during this time course (Figure 1E). TEM images showed that both hEROs-RPE and SD-RPE cells possessed specific microvilli and other normal cellular structures (Figure 1F), confirming the successful differentiation of hESC-RPE cells^[22,37].

Distribution and Quantity of Mitochondria in hEROs-RPE Cells TEM images were analyzed to determine the variations in mitochondrial distribution and quantity. Obviously, at day 60, mitochondria in both the hEROs-RPE and SD-RPE groups showed a perinuclear distribution (Figure 2A, 2B). Differentiation occurred at day 80, showing that hEROs-RPE mitochondria maintained their perinuclear distribution, while SD-RPE mitochondria were evenly distributed throughout the cell. The hEROs-RPE mitochondrial distribution changed evenly, with a more mature distribution at day 100 (Figure 2A, 2B). The distribution and morphological characteristics at day 120 and 140 were similar to those of their counterparts at day 100 and 160 (Figure 2A, 2B).

To assess the variations in mitochondrial quantity during RPE cell development, we labeled hESC-RPE cell mitochondria with MTG (Figure 2C) and performed semiquantitative analysis *via* flow cytometry (FCM)^[38]. The profile of mitochondrial quantity at different time points demonstrated that both the hEROs-RPE and SD-RPE groups showed significant increasing trends at the beginning (from day 60 to 80) and were subsequently maintained at this level (from day 80 to 160; Figure 2D, 2E). In addition, no significant differences in mitochondrial quantity were detected at any time point between hEROs-RPE and SD-RPE cells (Figure 2F). Representative flow histograms are also displayed (Figure 2G, 2H).

Ultrastructural Characteristics of Mitochondria in hEROs-RPE Cells The enlarged TEM images show the ultrastructural characteristics of hESC-RPE cell mitochondria, including cristae and length features. The cristae consisted of several invaginated inner mitochondrial membranes, which are associated with mitochondrial maturity^[39-41]. To better describe the variation in RPE cell mitochondria during the development process, cristae were observed at different time points *via* TEM (Figure 3A, 3B). Both hEROs-RPE and SD-RPE mitochondria showed scarce and discrete cristae at day 60, indicating immaturity. The SD-RPE mitochondria changed

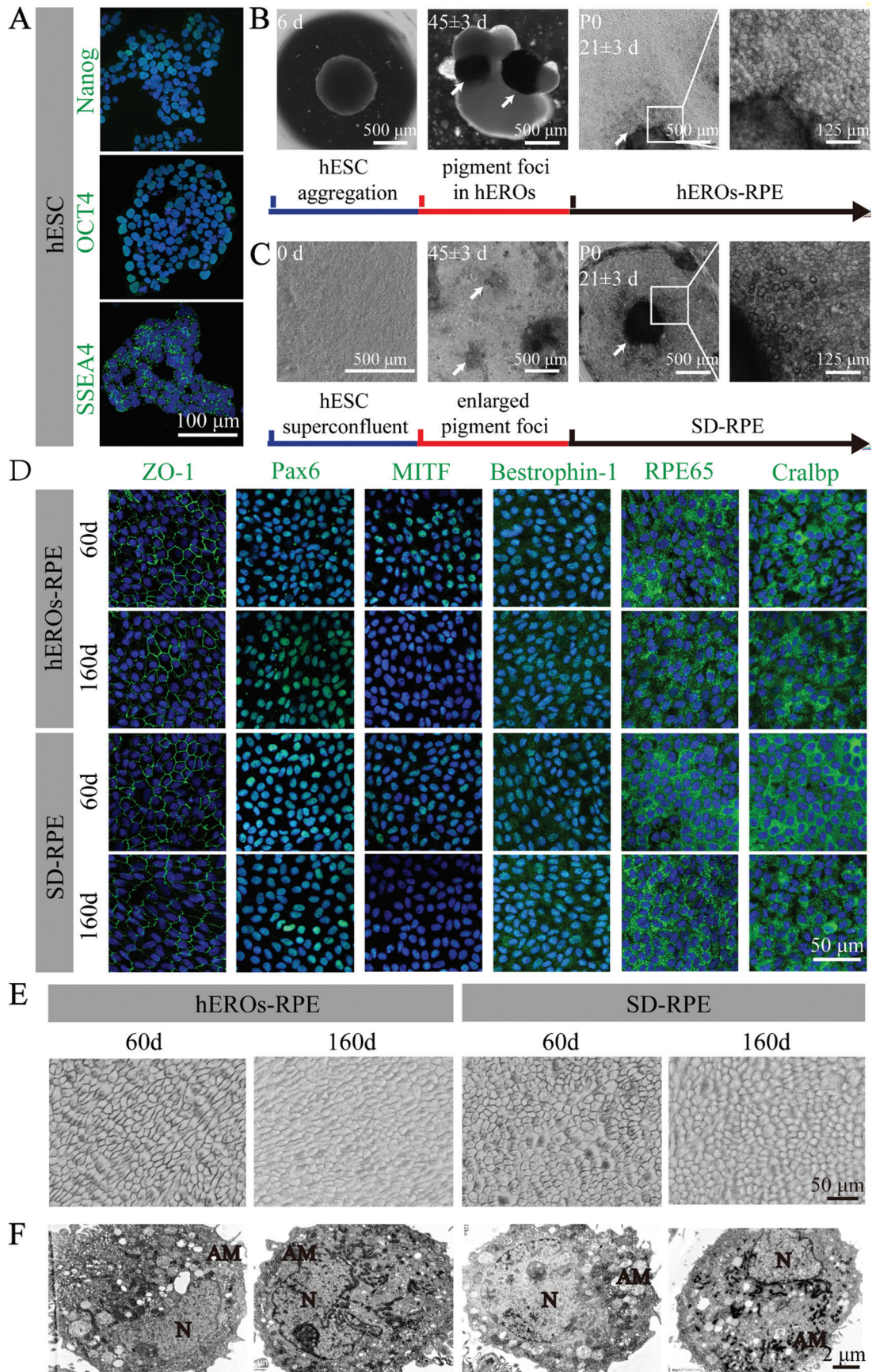


Figure 1 Generation and identification of hEROs-RPE and SD-RPE cells **A**: Immunofluorescence images of human embryonic stem cell (hESC) markers; **B**: Schematic of the hEROs-RPE cell differentiation protocol. White arrows showing pigment foci; **C**: Schematic of the SD-RPE cell differentiation protocol. White arrows showing pigment foci; **D**: Immunofluorescence images of hEROs-RPE and SD-RPE cells with RPE cell-specific markers at day 60 and 160; **E**: Light field images of hEROs-RPE and SD-RPE at day 60 and 160; **F**: TEM images of hEROs-RPE and SD-RPE cells at day 60 and 160; N: Nuclei; AM: Apical microvilli.

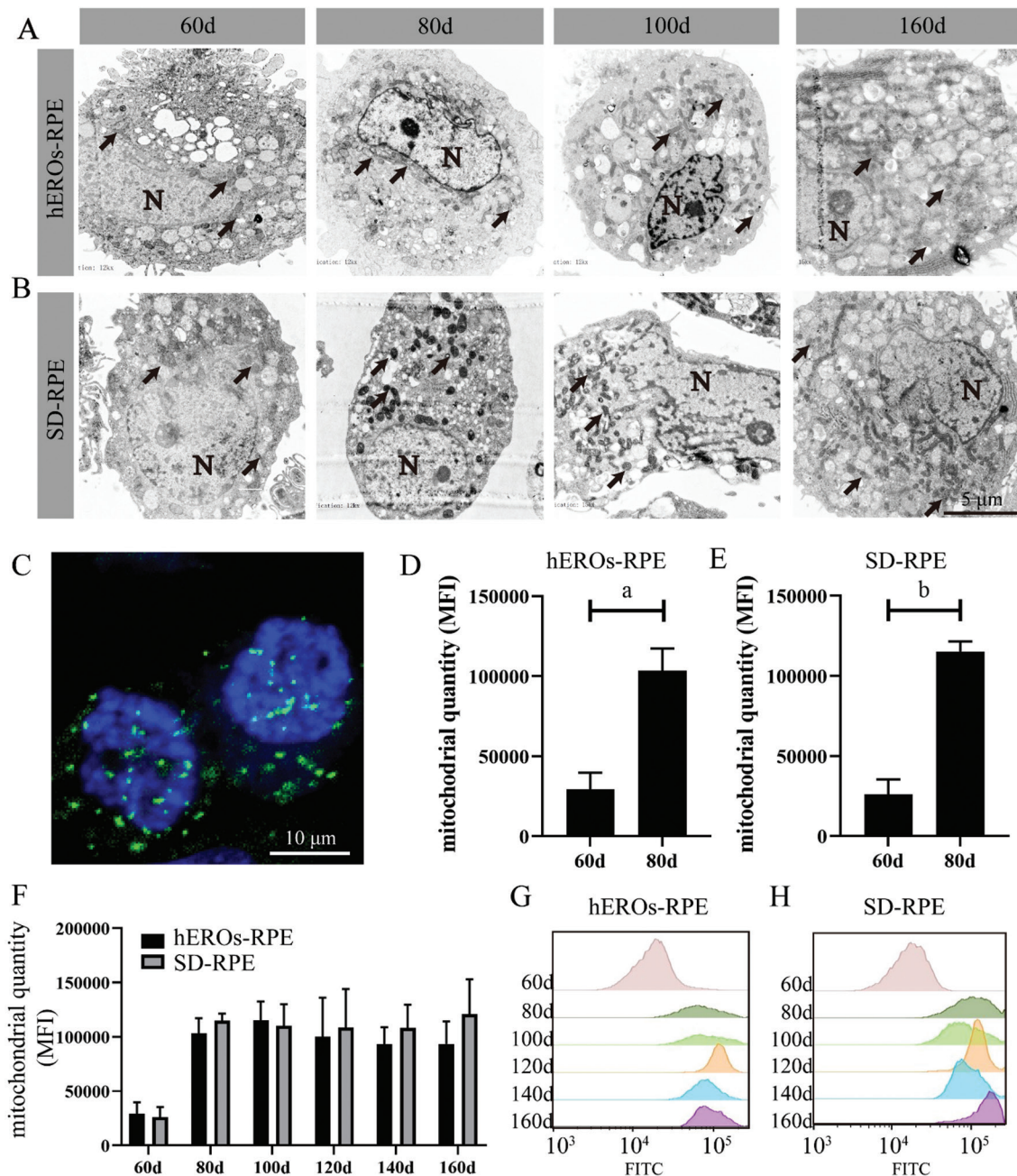


Figure 2 Mitochondrial distribution and quantity of hEROs-RPE and SD-RPE cells throughout development A, B: TEM images showing the cellular profiles. Black arrows showing mitochondria. N: Nuclei; C: hEROs-RPE mitochondria at day 100 stained with MitoTracker Green. D: The mitochondrial quantity in hEROs-RPE cells was significantly different at day 60 and 80. ^a $P < 0.05$, $n = 3$; E: The mitochondrial quantity in SD-RPE was significantly different at day 60 and 80. ^b $P < 0.01$, $n = 3$; F: The mitochondrial quantity variation in hEROs-RPE and SD-RPE cells, $n = 3$; G, H: Representative histograms corresponding to the mitochondrial quantities in hEROs-RPE and SD-RPE cells at different time points.

at day 80, at which point increased cristae were observed. However, the cristae in hEROs-RPE mitochondria were still immature currently point and did not reach maturity until day 100, at which point the cristae were abundant (Figure 3A, 3B). These results demonstrated that hEROs-RPE and SD-RPE mitochondria gradually became mature, as shown in the schematic diagram in Figure 3C.

Functional Variation in hEROs-RPE Mitochondria To assess the functional variation in the ability of mitochondria to

resist oxidative stress, the cellular ROS content and MMP at the physiological state were measured at every time point. The ROS level in both hEROs-RPE and SD-RPE cells was low at day 60, and two peaks emerged at day 80 and 160 (Figure 4A, 4C). The ROS level at different time points between day 60 and 160 differed significantly overall, but pairwise comparisons showed no difference in both RPE cell groups (Figure 4A, 4C), as shown by the typical flow histograms (Figure 4B, 4D). However, there were no significant differences in the ROS

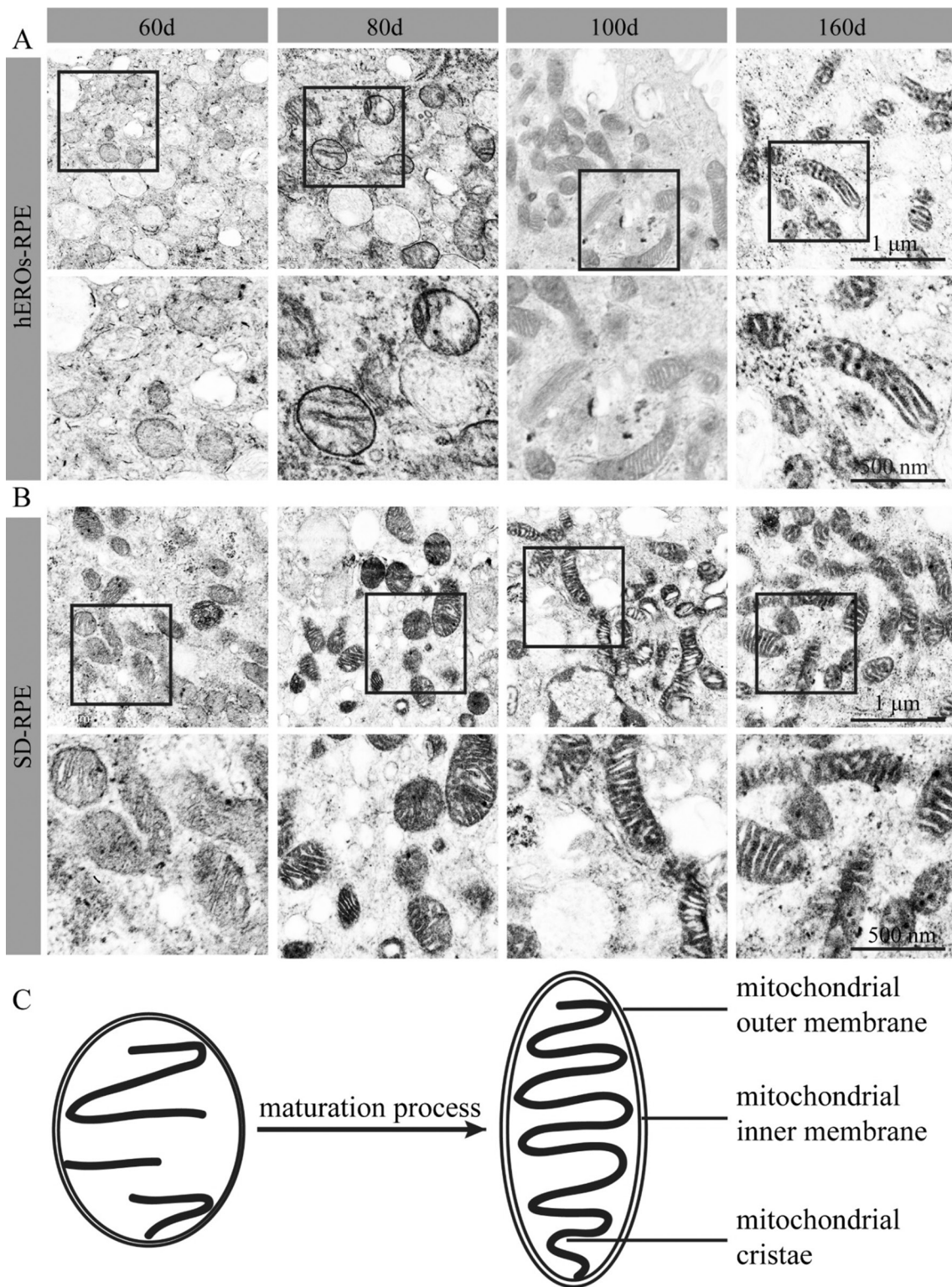


Figure 3 Variation of mitochondrial cristae and profiles of hEROs-RPE and SD-RPE cells at different time points A: The changes in hEROs-RPE mitochondrial cristae from day 60 to 160; B: The changes in SD-RPE mitochondrial cristae from day 60 to 160; C: An abridged general view of mitochondrial morphological variation.

contents in hEROs-RPE and SD-RPE cells at any time point (Figure 4E).

The MMP, determined by the ratio of red to green fluorescence, was measured by FCM after JC-1 staining. Although the cellular ROS content varied in the time frame analyzed, the MMP remained relatively stable in both groups (Figure

5A, 5B). In contrast to the ROS levels, the MMPs were not significantly different from day 60 to 160 (Figure 5C), and typical flow cytometry scatter plots are shown (Figure 5D, 5E). Meanwhile, their high-MMP subpopulations were counted (Figure 5F, 5G). The subpopulations with high MMPs decreased at only day 160 in both hEROs-RPE and SD-RPE cells.

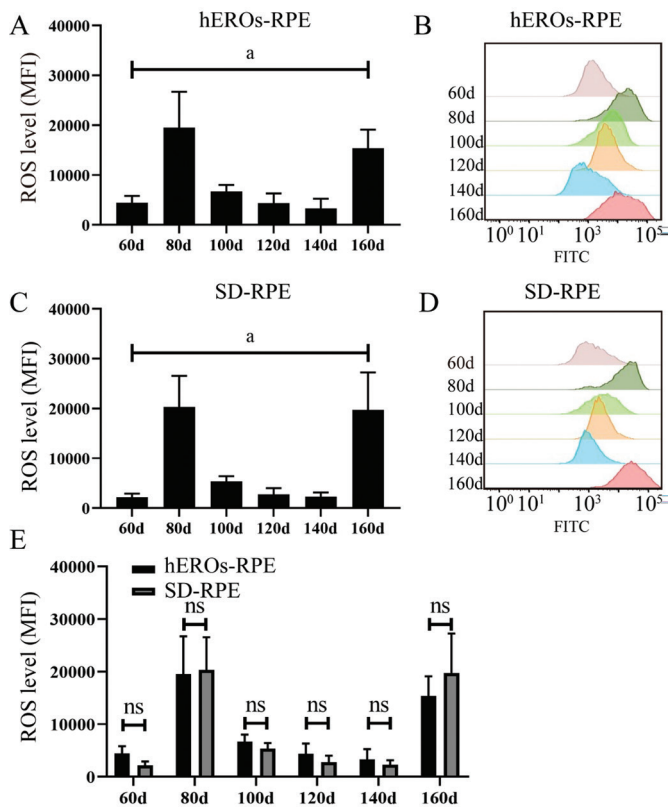


Figure 4 Variation in cellular ROS levels of hEROs-RPE and SD-RPE cells over time A: ROS variation in hEROs-RPE cells, $n=3$; B: Representative flow diagrams of hEROs-RPE cell ROS levels at different time points; C: ROS variation in SD-RPE cells, $n=3$; D: Representative flow diagrams of SD-RPE cell ROS levels at different time points; E: ROS levels at different time points were compared between hEROs-RPE and SD-RPE cells, $n=3$. $^aP\leq 0.05$.

The cellular ATP level was measured to determine the ability of hESC-RPE cell mitochondria to supply energy, revealing that the ATP levels in both hEROs-RPE and SD-RPE cells tended to first increase and then decrease, peaking at day 120 from day 60 to 160 individually (Figure 6A, 6B). Although the abilities to supply energy were similar between hEROs-RPE and SD-RPE mitochondria at day 120, the ATP content in hEROs-RPE cells was higher than that in SD-RPE cells at day 100 and 140 (Figure 6C), demonstrating their potential superior ability to supply energy. Moreover, the cellular ATP level in hEROs-RPE cells remained stable between day 120 to 140, while it dropped in SD-RPE cells during this time frame (Figure 6A, 6B).

DISCUSSION

Stem cell therapy has been a promising strategy for treating retinal degenerative diseases, such as AMD^[12,15,18]. While hESC-RPE cells have been widely studied in clinical trials for the treatment of AMD, methods for obtaining an optimized cell source and its biological characteristics, including mitochondria, have not been explored. This is the first systematic study on the mitochondrial characteristics of hERO-

RPE cells, and these results will hopefully facilitate the clinical application of hESC-RPE cells and subsequent mechanistic research on mitochondrial transfer.

Recently, SD-RPEs from hESCs or induced pluripotent stem cells (iPSCs) have been widely used in several clinical trials^[15,42-43]. Moreover, we previously established a new donor cell line, hEROs-RPEs, from hESCs that is very similar to human fetal RPE cells and shows promise for treating AMD^[22]. The general morphology and functional characteristics of both SD-RPE and hEROs-RPE cells have been studied, showing that hEROs-RPE cells are a better cell source and are advantageously more proliferative, and have a better ultrastructure, tight junction expression, and polarity. However, the mitochondrial characteristics of hEROs-RPE cells have rarely been researched. Thus, this study hopes to provide evidence for choosing optimized hEROs-RPE cells from the aspect of mitochondria. Since the RPE cell culture period is very long, cells from day 60 to 160 were selected for this study, covering the early, middle and later stages of hESC-RPE differentiation as well as the time point selected for clinical trials on SD-RPE cells (day 80)^[15]. Both morphological and functional indicators were used to evaluate the mitochondrial state at different time points.

Transplanted stem cells play an important role in rescuing degenerated retinal cells by differentiating to replace injured cells, supporting nutritional and anti-inflammatory effects by paracrine signaling as well as cellular exchange between donor and host cells^[44-46]. Mitochondrial transfer, as one method of cellular exchange and a new mechanism of stem cell therapy, has been widely studied. Although more than 40 organelles have been reported to be transported between cells^[24], mitochondria are of supreme cellular importance. This organelle with a two-lipid bilayer supplies energy and is responsible for cellular metabolism *via* respiration^[47]. Mitochondria are the site of numerous metabolic processes, such as cellular respiration and fat and amino acid metabolism^[27]. RPE cells are active in energy metabolism, which is supported by mitochondria^[48-50]. In addition, mitochondrial damage is a common pathophysiological process that occurs in a diverse array of diseases, especially degenerative diseases, including AMD^[51-52]. The release of accumulated ROS, unbalanced Ca^{2+} concentrations, and insufficient energy supply are key factors underlying mitochondrial damage, which then results in cell apoptosis and cell death in nearby areas^[53-57]. Mitochondrial structural damage and displacement have been observed in RPE cells from human donors with AMD^[58]. Enhanced levels of mitochondrial DNA lesions^[30] and decreased expression levels of electron transport chain proteins have been observed in the RPE cells of patients with AMD^[59-61]. Thus, treatments targeting RPE cell mitochondria in patients with AMD are

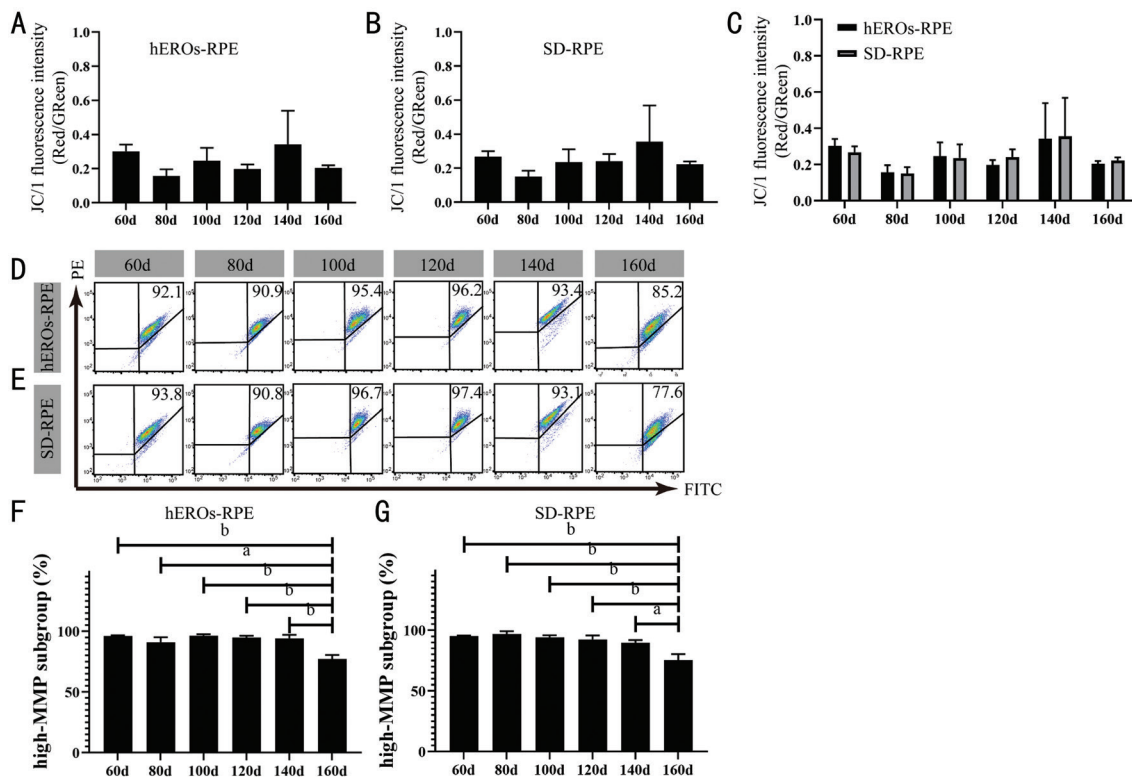


Figure 5 The MMP remained relatively stable in both hEROs-RPE and SD-RPE cells A, B: The MMP variation in hEROs-RPE and SD-RPE cells, $n=3$; C: The MMPs of hEROs-RPE and SD-RPE cells were compared at different time points, $n=3$; D, E: Representative flow charts of MMPs in hEROs-RPE and SD-RPE cells at different time points; F, G: The high-MMP subgroups at day 160 were much lower than those at other time points in both hEROs-RPE and SD-RPE cells, $n=3$. ^a $P\leq 0.05$; ^b $P\leq 0.01$.

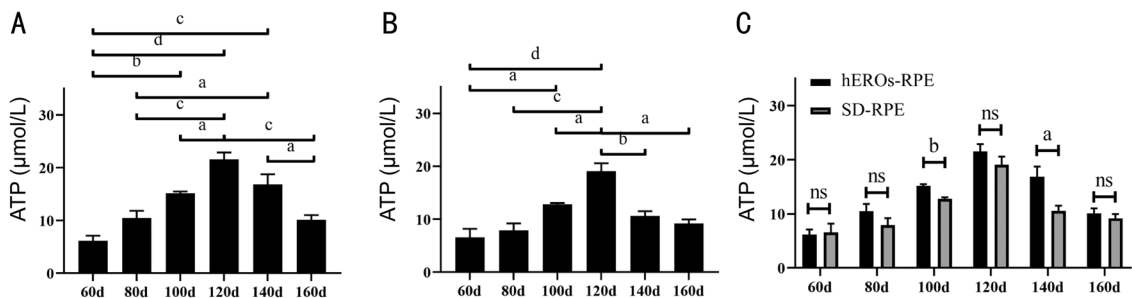


Figure 6 Variation in cellular ATP levels of hEROs-RPE and SD-RPE cells over time A, B: Variation in hEROs-RPE and SD-RPE cellular ATP contents, $n=3$; ^a $P\leq 0.05$; ^b $P\leq 0.01$; ^c $P\leq 0.001$; ^d $P\leq 0.0001$; C: The ATP contents were compared between hEROs-RPE and SD-RPE at different time points. Day 100, ^b $P\leq 0.01$; day 140, ^a $P\leq 0.05$, $n=3$.

highly desirable. Mitochondrial transfer occurs between stem cells and retinal cells, including RPE cells^[34], and is capable of rescuing the mitochondrial function of injured RPE cells. Investigating the mitochondrial characteristics of RPE seed cells and determining the optimal time point for obtaining high-quality hESC-RPEs are vital.

The mitochondrial ultrastructure is reportedly different between undifferentiated stem cells and terminally differentiated cells^[27,62-63]. TEM images show that mitochondria of human and mouse ESCs are immature, globular, rare, and perinuclear^[62-69]. In addition, the cristae of most organisms are tubular or baggy and connect to the mitochondrial inner membrane by fine tubular connections^[70], which can reflect mitochondrial

maturity, while stem cells exhibit fewer and underdeveloped mitochondrial cristae^[39-41]. During the process of differentiation, mitochondrial cristae become more mature and multiply^[18]. This phenomenon was observed during the development of hEROs-RPE and SD-RPE cells in this study. Both hEROs-RPE and SD-RPE cells showed relatively immature mitochondrial development at day 60, as indicated by lower mitochondrial quantities, globular appearances, perinuclear distributions, and rare cristae. Although their mitochondrial quantity peaked simultaneously at day 80, hEROs-RPE mitochondria manifested more immature morphological characteristics than SD-RPE mitochondria and sustained their characteristics of a more globular morphology, perinuclear distribution, and rare

and discrete cristae. This result is in line with our previous study showing that hEROs-RPE cells might develop slower than SD-RPE cells^[22].

The cellular ROS and MMP levels were measured to show mitochondrial functions under physiological conditions. Immature mitochondria produce low levels of ROS^[67,71], and the ROS levels in both hEROs-RPE and SD-RPE cells peaked twice at day 80 and 160. The first peak corresponded with the time point at which the mitochondrial quantity peaked, indicating that the high ROS content was due to mitochondrial biogenesis. However, the second peak was probably caused by cellular senescence. Compared to the mitochondria of young cells, the mitochondria of aging cells could produce more ROS. Aging cells were more sensitive to ROS, too. Additionally, excess ROS from mitochondria was significant since it could do more harm to mitochondria and then threaten the health of RPE cells. Evidence supports that the decrease of MMP stimulates the leakage of ROS to the cytoplasm. As well, the decrease of MMP was considered a sign of cell apoptosis, so a healthy MMP was important for the function of mitochondria. The MMP remained relatively stable during this time, indicating that the cells were healthy when cultured for day 160. However, the high-MMP subgroup at day 160 was much lower than that any other time point, indicating the possibility of cell over-maturation. In addition, cells require energy to run reactions that maintain their viability, growth, and proper function, and ATP is the dominant chemical energy currency in cells^[72]. The cellular ATP content signifies the ability of mitochondria to supply energy, and a high ATP content indicates that mitochondria function well. Cellular ATP levels peaked at day 120 in both hEROs-RPE and SD-RPE cells; the hEROs-RPE cells maintained a high ATP content for day 140, whereas the level in SD-RPE cells decreased sooner. From these data, we can draw conclusions regarding an optimized time window for obtaining hEROs-RPE cells. In summary, hEROs-RPE mitochondria developed slower than their SD counterparts, which was consistent with the slower development of hEROs-RPE cells compared to SD-RPE cells. hEROs-RPE mitochondria matured at day 100, whereas SD-RPE mitochondria matured at day 80, as determined by morphological analysis. However, both cell lines exhibited high ROS levels at day 80, which is not an ideal scenario for transplantation therapy. In our study, both hEROs-RPE and SD-RPE cells showed low levels of ROS from day 100 to 140 and maintained a normal MMP during this period. Regarding energy supply, hEROs-RPE mitochondria were better than SD-RPE mitochondria since they maintained high ATP levels for a longer period. Since mitochondrial transfer is an active process that is probably and mainly mediated by the ATP supply^[73-74], a high cellular ATP content is more serviceable. Considering

all these data, culturing hEROs-RPE cells for day 100 to 140 is better from a mitochondrial viewpoint.

In summary, this study systemically investigated the temporal mitochondrial characteristics of SD-RPE and hEROs-RPE cells and determined that hEROs-RPE cells from day 100 to 140 are an optimal cell source for treating AMD. However, the role of hEROs-RPE cells in the treatment of AMD *in vivo* and many issues regarding mitochondrial transfer in stem cell therapy still need to be further explored.

ACKNOWLEDGEMENTS

We would like to express our gratitude to Dr. Yuan Gao and Dr. Haiwei Xu at the Southwest Hospital/Southwest Eye Hospital of Third Military Medical University (Army Medical University) for their assistance and support. We also would like to thank Dr. Jie Hao in State Key Laboratory of Stem Cells and Reproductive Biology, Institute of Zoology, Chinese Academy of Sciences for providing the hESC cell line Q-CTS-hESC-2.

Foundations: Supported by the National Key Research and Development Program of China (No.2018YFA01017302); the National Natural Science Foundation of China (No.82000945).

Conflicts of Interest: Xu HJ, None; Li QY, None; Zou T, None; Yin ZQ, None.

REFERENCES

- 1 Bertolotti E, Neri A, Camparini M, Macaluso C, Marigo V. Stem cells as source for retinal pigment epithelium transplantation. *Prog Retin Eye Res* 2014;42:130-144.
- 2 Congdon N, O'Colmain B, Klaver CC, Klein R, Muñoz B, Friedman DS, Kempen J, Taylor HR, Mitchell P, Eye Diseases Prevalence Research Group. Causes and prevalence of visual impairment among adults in the United States. *Arch Ophthalmol* 2004;122(4):477-485.
- 3 Wong WL, Su XY, Li X, Cheung CMG, Klein R, Cheng CY, Wong TY. Global prevalence of age-related macular degeneration and disease burden projection for 2020 and 2040: a systematic review and meta-analysis. *Lancet Glob Heal* 2014;2(2):e106-e116.
- 4 Song P, Du Y, Chan KY, Theodoratou E, Rudan I. The national and subnational prevalence and burden of age-related macular degeneration in China. *J Glob Health* 2017;7(2):020703.
- 5 Brown MM, Brown GC, Stein JD, Roth Z, Campanella J, Beauchamp GR. Age-related macular degeneration: economic burden and value-based medicine analysis. *Can J Ophthalmol* 2005;40(3):277-287.
- 6 Wysong A, Lee PP, Sloan FA. Longitudinal incidence of adverse outcomes of age-related macular degeneration. *Arch Ophthalmol* 2009;127(3):320-327.
- 7 Augustin A, Sahel JA, Bandello F, Dardennes R, Maurel F, Negrini C, Hieke K, Berdeaux G. Anxiety and depression prevalence rates in age-related macular degeneration. *Invest Ophthalmol Vis Sci* 2007;48(4):1498-1503.

- 8 Brody BL, Gamst AC, Williams RA, Smith AR, Lau PW, Dolnak D, Rapoport MH, Kaplan RM, Brown SI. Depression, visual acuity, comorbidity, and disability associated with age-related macular degeneration. *Ophthalmology* 2001;108(10):1893-1900; discussion 1900.
- 9 Berman K, Brodaty H. Psychosocial effects of age-related macular degeneration. *Int Psychogeriatr* 2006;18(3):415-428.
- 10 Fröhlich E, Klessen C. Regional differences and post-mortem stability of enzymatic activities in the retinal pigment epithelium. *Graefes Arch Clin Exp Ophthalmol* 2003;241(5):385-393.
- 11 Datta S, Cano M, Ebrahimi K, Wang L, Handa JT. The impact of oxidative stress and inflammation on RPE degeneration in non-neovascular AMD. *Prog Retin Eye Res* 2017;60:201-218.
- 12 da Cruz L, Fynes K, Georgiadis O, et al. Phase 1 clinical study of an embryonic stem cell-derived retinal pigment epithelium patch in age-related macular degeneration. *Nat Biotechnol* 2018;36(4):328-337.
- 13 Kamao H, Mandai M, Okamoto S, Sakai N, Suga A, Sugita S, Kiryu J, Takahashi M. Characterization of human induced pluripotent stem cell-derived retinal pigment epithelium cell sheets aiming for clinical application. *Stem Cell Reports* 2014;2(2):205-218.
- 14 Li Y, Tsai YT, Hsu CW, Erol D, Yang J, Wu WH, Davis RJ, Egli D, Tsang SH. Long-term safety and efficacy of human-induced pluripotent stem cell (iPS) grafts in a preclinical model of retinitis pigmentosa. *Mol Med* 2012;18:1312-1319.
- 15 Liu Y, Xu HW, Wang L, Li SY, Zhao CJ, Hao J, Li QY, Zhao TT, Wu W, Wang Y, Zhou Q, Qian C, Wang L, Yin ZQ. Human embryonic stem cell-derived retinal pigment epithelium transplants as a potential treatment for wet age-related macular degeneration. *Cell Discov* 2018;4:50.
- 16 Lu B, Malcuit C, Wang S, Girman S, Francis P, Lemieux L, Lanza R, Lund R. Long-term safety and function of RPE from human embryonic stem cells in preclinical models of macular degeneration. *Stem Cells* 2009;27(9):2126-2135.
- 17 Schwartz SD, Hubschman JP, Heilwell G, Franco-Cardenas V, Pan CK, Ostrick RM, Mickunas E, Gay R, Klimanskaya I, Lanza R. Embryonic stem cell trials for macular degeneration: a preliminary report. *Lancet* 2012;379(9817):713-720.
- 18 Song WK, Park KM, Kim HJ, Lee JH, Choi J, Chong SY, Shim SH, Del Priore LV, Lanza R. Treatment of macular degeneration using embryonic stem cell-derived retinal pigment epithelium: preliminary results in Asian patients. *Stem Cell Reports* 2015;4(5):860-872.
- 19 Jensen C, Teng Y. Is it time to start transitioning from 2D to 3D cell culture? *Front Mol Biosci* 2020;7:33.
- 20 Ben M'Barek K, Habeler W, Monville C. Stem cell-based RPE therapy for retinal diseases: engineering 3D tissues amenable for regenerative medicine. *Adv Exp Med Biol* 2018;1074:625-632.
- 21 Jin ZB, Gao ML, Deng WL, Wu KC, Sugita S, Mandai M, Takahashi M. Stemming retinal regeneration with pluripotent stem cells. *Prog Retin Eye Res* 2019;69:38-56.
- 22 Wu W, Zeng Y, Li Z, Li Q, Xu H, Yin ZQ. Features specific to retinal pigment epithelium cells derived from three-dimensional human embryonic stem cell cultures - a new donor for cell therapy. *Oncotarget* 2016;7(16):22819-22833.
- 23 Gonzalez-Cordero A, West EL, Pearson RA, Duran Y, Carvalho LS, Chu CJ, Naeem A, Blackford SJI, Georgiadis A, Lakowski J, Hubank M, Smith AJ, Bainbridge JWB, Sowden JC, Ali RR. Photoreceptor precursors derived from three-dimensional embryonic stem cell cultures integrate and mature within adult degenerate retina. *Nat Biotechnol* 2013;31(8):741-747.
- 24 Rogers RS, Bhattacharya J. When cells become organelle donors. *Physiol Bethesda Md* 2013;28(6):414-422.
- 25 Dyer MA. Biomedicine: an eye on retinal recovery. *Nature* 2016;540(7633):350-351.
- 26 Zou T, Gao L, Zeng Y, Li Q, Li Y, Chen S, Hu X, Chen X, Fu C, Xu H, Yin ZQ. Organoid-derived C-Kit⁺/SSEA4⁺ human retinal progenitor cells promote a protective retinal microenvironment during transplantation in rodents. *Nat Commun* 2019;10(1):1205.
- 27 Loureiro R, Mesquita KA, Magalhães-Novais S, Oliveira PJ, Vega-Naredo I. Mitochondrial biology in cancer stem cells. *Semin Cancer Biol* 2017;47:18-28.
- 28 Natarajan V, Chawla R, Mah T, Vivekanandan R, Tan SY, Sato PY, Mallilankaraman K. Mitochondrial dysfunction in age-related metabolic disorders. *Proteomics* 2020;20(5-6):e1800404.
- 29 Ao J, Wood JP, Chidlow G, Gillies MC, Casson RJ. Retinal pigment epithelium in the pathogenesis of age-related macular degeneration and photobiomodulation as a potential therapy? *Clin Exp Ophthalmol* 2018;46(6):670-686.
- 30 Terluk MR, Kapphahn RJ, Soukup LM, Gong H, Gallardo C, Montezuma SR, Ferrington DA. Investigating mitochondria as a target for treating age-related macular degeneration. *J Neurosci* 2015;35(18):7304-7311.
- 31 Hsu YC, Wu YT, Yu TH, Wei YH. Mitochondria in mesenchymal stem cell biology and cell therapy: from cellular differentiation to mitochondrial transfer. *Semin Cell Dev Biol* 2016;52:119-131.
- 32 Lim GB. Intracoronary mitochondrial transplantation. *Nat Rev Cardiol* 2020;17(3):131.
- 33 Fang SY, Roan JN, Lee JS, Chiu MH, Lin MW, Liu CC, Lam CF. Transplantation of viable mitochondria attenuates neurologic injury after spinal cord ischemia. *J Thorac Cardiovasc Surg* 2021;161(5):e337-e347.
- 34 Jiang D, Chen FX, Zhou H, Lu YY, Tan H, Yu SJ, Yuan J, Liu H, Meng WX, Jin ZB. Bioenergetic crosstalk between mesenchymal stem cells and various ocular cells through the intercellular trafficking of mitochondria. *Theranostics* 2020;10(16):7260-7272.
- 35 Gu Q, Wang J, Wang L, Liu ZX, Zhu WW, Tan YQ, Han WF, Wu J, Feng CJ, Fang JH, Liu L, Wang L, Li W, Zhao XY, Hu BY, Hao J, Zhou Q. Accreditation of biosafe clinical-grade human embryonic stem cells according to Chinese regulations. *Stem Cell Rep* 2017;9(1):366-380.
- 36 Kuwahara A, Ozone C, Nakano T, Saito K, Eiraku M, Sasai Y. Generation of a ciliary margin-like stem cell niche from self-organizing human retinal tissue. *Nat Commun* 2015;6:6286.

- 37 Li QY, Zou T, Gong Y, Chen SY, Zeng YX, Gao LX, Weng CH, Xu HW, Yin ZQ. Functional assessment of cryopreserved clinical grade hESC-RPE cells as a qualified cell source for stem cell therapy of retinal degenerative diseases. *Exp Eye Res* 2021;202:108305.
- 38 Ho TT, Warr MR, Adelman ER, Lansinger OM, Flach J, Verovskaya EV, Figueroa ME, Passequé E. Autophagy maintains the metabolism and function of young and old stem cells. *Nature* 2017;543(7644):205-210.
- 39 Sathananthan H, Pera M, Trounson A. The fine structure of human embryonic stem cells. *Reproductive Biomed Online* 2002;4(1):56-61.
- 40 Oh SK, Kim HS, Ahn HJ, Seol HW, Kim YY, Park YB, Yoon CJ, Kim DW, Kim SH, Moon SY. Derivation and characterization of new human embryonic stem cell lines: SNUhES1, SNUhES2, and SNUhES3. *Stem Cells* 2005;23(2):211-219.
- 41 Cho YM, Kwon S, Pak YK, Seol HW, Choi YM, Park DJ, Park KS, Lee HK. Dynamic changes in mitochondrial biogenesis and antioxidant enzymes during the spontaneous differentiation of human embryonic stem cells. *Biochem Biophys Res Commun* 2006;348(4):1472-1478.
- 42 Sowden JC. ESC-derived retinal pigmented epithelial cell transplants in patients: so far, so good. *Cell Stem Cell* 2014;15(5):537-538.
- 43 Mandai M, Watanabe A, Kurimoto Y, et al. Autologous induced stem-cell-derived retinal cells for macular degeneration. *N Engl J Med* 2017;376(11):1038-1046.
- 44 Aghajani Nargesi A, Lerman LO, Eirin A. Mesenchymal stem cell-derived extracellular vesicles for kidney repair: current status and looming challenges. *Stem Cell Res Ther* 2017;8(1):273.
- 45 Borbolla JR, López-Hernández MA, De Diego J, González-Avante M, Trueba E, Collados MT. Use of interleukin-11 after autologous stem cell transplant: report of three cases and a very brief review of the literature. *Haematologica* 2001;86(8):891-892.
- 46 Lozano-Elena F, Planas-Riverola A, Vilarrasa-Blasi J, Schwab R, Caño-Delgado AI. Paracrine brassinosteroid signaling at the stem cell niche controls cellular regeneration. *J Cell Sci* 2017.
- 47 Lane N, Martin W. The energetics of genome complexity. *Nature* 2010;467(7318):929-934.
- 48 Zhao C, Yasumura D, Li X, Matthes M, Lloyd M, Nielsen G, Ahern K, Snyder M, Bok D, Dunaief JL, LaVail MM, Vollrath D. mTOR-mediated dedifferentiation of the retinal pigment epithelium initiates photoreceptor degeneration in mice. *J Clin Invest* 2011;121(1):369-383.
- 49 Rohrer B, Bandyopadhyay M, Beeson C. Reduced metabolic capacity in aged primary retinal pigment epithelium (RPE) is correlated with increased susceptibility to oxidative stress. *Adv Exp Med Biol* 2016;854:793-798.
- 50 Adijanto J, Philp NJ. Cultured primary human fetal retinal pigment epithelium (hfRPE) as a model for evaluating RPE metabolism. *Exp Eye Res* 2014;126:77-84.
- 51 Golestaneh N, Chu Y, Xiao YY, Stoleru GL, Theos AC. Dysfunctional autophagy in RPE, a contributing factor in age-related macular degeneration. *Cell Death Dis* 2017;8(1):e2537.
- 52 Fisher CR, Ferrington DA. Perspective on AMD pathobiology: a bioenergetic crisis in the RPE. *Invest Ophthalmol Vis Sci* 2018;59(4):AMD41-AMD47.
- 53 Murphy MP. How mitochondria produce reactive oxygen species. *Biochem J* 2009;417(1):1-13.
- 54 Hamanaka RB, Chandel NS. Mitochondrial reactive oxygen species regulate cellular signaling and dictate biological outcomes. *Trends Biochem Sci* 2010;35(9):505-513.
- 55 Chernorudskiy AL, Zito E. Regulation of calcium homeostasis by ER redox: a close-up of the ER/mitochondria connection. *J Mol Biol* 2017;429(5):620-632.
- 56 Chen J, Mehta JL, Haider N, Zhang X, Narula J, Li D. Role of caspases in Ox-LDL-induced apoptotic cascade in human coronary artery endothelial cells. *Circ Res* 2004;94(3):370-376.
- 57 Reubold TF, Eschenburg S. A molecular view on signal transduction by the apoptosome. *Cell Signal* 2012;24(7):1420-1425.
- 58 Bianchi E, Scarinci F, Ripandelli G, Feher J, Pacella E, Magliulo G, Gabrieli CB, Plateroti R, Plateroti P, Mignini F, Artico M. Retinal pigment epithelium, age-related macular degeneration and neurotrophic keratouveitis. *Int J Mol Med* 2013;31(1):232-242.
- 59 Feher J, Kovacs I, Artico M, Cavallotti C, Papale A, Balacco Gabrieli C. Mitochondrial alterations of retinal pigment epithelium in age-related macular degeneration. *Neurobiol Aging* 2006;27(7):983-993.
- 60 Nordgaard CL, Berg KM, Kapphahn RJ, Reilly C, Feng X, Olsen TW, Ferrington DA. Proteomics of the retinal pigment epithelium reveals altered protein expression at progressive stages of age-related macular degeneration. *Invest Ophthalmol Vis Sci* 2006;47(3):815-822.
- 61 Nordgaard CL, Karunadharm PP, Feng X, Olsen TW, Ferrington DA. Mitochondrial proteomics of the retinal pigment epithelium at progressive stages of age-related macular degeneration. *Invest Ophthalmol Vis Sci* 2008;49(7):2848-2855.
- 62 Lonergan T, Brenner C, Bavister B. Differentiation-related changes in mitochondrial properties as indicators of stem cell competence. *J Cell Physiol* 2006;208(1):149-153.
- 63 Vega-Naredo I, Loureiro R, Mesquita KA, Barbosa IA, Tavares LC, Branco AF, Erickson JR, Holy J, Perkins EL, Carvalho RA, Oliveira PJ. Mitochondrial metabolism directs stemness and differentiation in P19 embryonal carcinoma stem cells. *Cell Death Differ* 2014;21(10):1560-1574.
- 64 Peiris-Pagès M, Martínez-Outschoorn UE, Pestell RG, Sotgia F, Lisanti MP. Cancer stem cell metabolism. *Breast Cancer Res* 2016;18(1):55.
- 65 St John JC, Ramalho-Santos J, Gray HL, Petrosko P, Rawe VY, Navara CS, Simerly CR, Schatten GP. The expression of mitochondrial DNA transcription factors during early cardiomyocyte *in vitro* differentiation from human embryonic stem cells. *Cloning Stem Cells* 2005;7(3):141-153.
- 66 Mandal S, Lindgren AG, Srivastava AS, Clark AT, Banerjee U. Mitochondrial function controls proliferation and early differentiation potential of embryonic stem cells. *Stem Cells* 2011;29(3):486-495.
- 67 Prigione A, Fauler B, Lurz R, Lehrach H, Adjaye J. The senescence-related mitochondrial/oxidative stress pathway is repressed in human induced pluripotent stem cells. *Stem Cells* 2010;28(4):721-733.

Mitochondrial properties of hEROs-RPE cells

- 68 Varum S, Rodrigues AS, Moura MB, Momcilovic O, Easley CA, Ramalho-Santos J, Van Houten B, Schatten G. Energy metabolism in human pluripotent stem cells and their differentiated counterparts. *PLoS One* 2011;6(6):e20914.
- 69 Prowse AB, Chong F, Elliott DA, Elefanty AG, Stanley EG, Gray PP, Munro TP, Osborne GW. Analysis of mitochondrial function and localisation during human embryonic stem cell differentiation *in vitro*. *PLoS One* 2012;7(12):e52214.
- 70 Frey TG, Renken CW, Perkins GA. Insight into mitochondrial structure and function from electron tomography. *Biochim Biophys Acta* 2002;1555(1-3):196-203.
- 71 Gammon L, Biddle A, Heywood HK, Johannessen AC, MacKenzie IC. Sub-sets of cancer stem cells differ intrinsically in their patterns of oxygen metabolism. *PLoS One* 2013;8(4):e62493.
- 72 Mookerjee SA, Gerencser AA, Nicholls DG, Brand MD. Quantifying intracellular rates of glycolytic and oxidative ATP production and consumption using extracellular flux measurements. *J Biol Chem* 2017;292(17):7189-7207.
- 73 Spees JL, Olson SD, Whitney MJ, Prockop DJ. Mitochondrial transfer between cells can rescue aerobic respiration. *Proc Natl Acad Sci U S A* 2006;103(5):1283-1288.
- 74 Gurke S, Barroso JFV, Hodneland E, Bukoreshtliev NV, Schlicker O, Gerdes HH. Tunneling nanotube (TNT)-like structures facilitate a constitutive, actomyosin-dependent exchange of endocytic organelles between normal rat kidney cells. *Exp Cell Res* 2008; 314(20):3669-3683.